GRB 060218/SN 2006aj: prompt emission from inverse-Compton scattering of shock breakout thermal photons

Z. G. Dai[1,2], Bing Zhang[2], and E. W. Liang[2,3]

[1]*Department of Astronomy, Nanjing University, Nanjing 210093, China*
[2]*Department of Physics, University of Nevada, Las Vegas, NV 89154, USA*
[3]*Department of Physics, Guangxi University, Nanning 530004, China*

ABSTRACT

The γ-ray burst (GRB) 060218/SN 2006aj is a peculiar event, with the second lowest redshift, low luminosity, long duration, chromatic lightcurve features, and in particular, the presence of a thermal component in the X-ray and UV-optical spectra. Thanks to detailed temporal and spectral coverage of the *Swift* observatory, the abundant data allow the GRB prompt emission to be modelled in great detail for the first time. The low flux of prompt UV/optical emission disfavors the conventional internal shock/synchrotron radiation models, which generally predict strong UV/optical emission. Here we show that the unusual prompt emission of GRB 060218 can be produced by inverse-Compton scattering of shock-accelerated relativistic electrons off the detected thermal photons. A pair of (forward plus reverse) shocks form when a relativistic outflow interacts with a preexisting slower shell. The observed γ-ray emission and X-ray emission arise from the reverse-shocked and forward-shocked regions, respectively. A fit to the data requires an initially increasing outflow luminosity, which is consistent with the prediction of the popular collapsar model.

Subject headings: gamma-rays: bursts — relativity — shock waves

1. Introduction

The γ-ray burst (GRB) 060218 was detected by the Burst Alert Telescope (BAT) onboard *Swft* satellite on 2006 February 18.149 UT (Cusumano et al. 2006). The prompt γ-ray emission lasted about 2000 s and thus it is one of the longest GRBs. Spectroscopic measurements after the burst revealed that this event was associated with a type-Ic supernova, SN 2006aj (Modjaz et al. 2006; Pian et al. 2006; Sollerman et al. 2006; Mirabal et al. 2006; Cobb et al. 2006) and that its redshift is $z = 0.0331$ (Mirabal & Halpern 2006). This is the

second lowest redshift GRB after GRB 980425/SN 1998bw. The burst has several unusual γ-ray and X-ray properties (Campana et al. 2006, see Fig.1). First, both prompt γ-ray emission and X-ray emission detected by BAT and the X-ray Telescope (XRT) exhibit a slow brightening and a final steep decay, unlike spiky light curves of classical bursts at higher redshifts. The lightcurves are chromatic, with the gamma-rays fading up earlier than X-rays. Second, the peak γ-ray flux is as low as $\sim 10^{-8}\,{\rm erg\,cm^{-2}\,s^{-1}}$ and the isotropic-equivalent γ-ray energy is a few times 10^{49} ergs, about three orders of magnitude lower than the typical energy of classical GRBs. Third, a soft thermal component was detected by XRT ~ 300 to 10^4 s after the burst, which a luminosity $\sim 10^{46}\,{\rm erg\,s^{-1}}$. The thermal component is also identified in the UVOT data at $\sim 10^5$ s. This soft component is likely due to the breakout of a radiation-dominated shock, possibly driven by a cocoon (Mészáros & Rees 2001; Ramirez-Ruiz et al. 2002; Zhang et al. 2003), parts of uncorked envelope matter (Waxman & Mészáros 2003) or parts of accelerated envelope matter (Colgate 1974; Tan et al. 2001). Fourth, the prompt optical/UV emission is extremely faint and its flux is about five orders of magnitude fainter than that of the prompt X-ray emission. Finally, it is interesting to note that the observed X-ray afterglow decayed as a simple power law with time ($\sim t^{-1.2}$) up to 10 days after the burst.

In the conventional internal shock models (for reviews see Zhang & Mészáros 2004 and Piran 2005), collisions among relativistic shells with different Lorentz factors would lead to internal shocks and the prompt emission of a GRB could arise from shock-accelerated electrons by synchrotron radiation and/or inverse-Compton scattering (e.g. Rees & Mészáros 1994; Dai & Lu 2002; Zhang & Mészáros 2002). In these models, the typical synchrotron self-absorption frequency is in the optical/UV band, so the prompt optical/UV emission flux is about three orders of magnitude fainter than the prompt X-ray flux because the synchrotron spectrum is $\nu F_\nu \propto \nu^{4/3}$ in the optical/UV to X-ray bands. The models predict a strong prompt optical/UV flash (Mészáros & Rees 1999), especially in low-redshift bursts. The tight constraints of the prompt UV-optical data of GRB 060218 therefore implies that the conventional internal shocks/synchrotron radiation models are inapplicable at least for this burst.

In this Letter, we propose a model in which a relativistic outflow interacts with a preexisting slower shell, leading to a pair of relativistic (forward plus reverse) shocks. The slower shell could have been a part of the stellar envelope ejected from the central engine prior to the GRB or a circum-burst dense clumpy cloud. We show that the unusual prompt emission of GRB 060218 could be produced by inverse-Compton (IC) scattering of shock-accelerated electrons off the detected shock breakout thermal photons. To our knowledge, this is the first detailed theoretical model of the prompt emission of a GRB, which is made possible thanks to the broad temporal and spectral coverage of GRB 060218 by the *Swift*

satellite. In §2 we present the IC spectrum of a relativistic shock in a general case. In §3 we discuss the shock dynamics and calculate the emission luminosity and in §4 we constrain the model parameters for GRB 060218. Our results are summarized in §5.

2. IC spectrum in relativistic shocks

We first discuss a general case in which a relativistic shock with bulk Lorentz factor of γ occurs simultaneously with a soft photon source. We assume that the luminosity of this photon source is L_0 and its radius is much smaller than the shock radius R. We now consider IC scattering of the shock-accelerated electrons with the soft photons. If the shock expands outwards isotropically, there should be many head-on scatterings between the electrons and the soft photons so that some electrons would quickly cool down, as argued by Brunetti (2000), Wang, Li & Mészáros (2006), Wang & Mészáros (2006), and Fan & Piran (2006). Letting ϵ_0 be the typical energy of the soft photons in the observer's frame, we have the IC power and characteristic energy from a relativistic electron with Lorentz factor γ_e,

$$P(\gamma_e) = \sigma_T c \gamma^2 \gamma_e^2 U_0', \tag{1}$$

$$\epsilon_\gamma(\gamma_e) = \gamma_e^2 \epsilon_0. \tag{2}$$

The factor γ^2 in eq. (1) is introduced to transform the power in the shock rest frame to the observer's frame, σ_T is the Thomson cross section, and $U_0' = L_0/(4\pi R^2 \gamma^2 c)$ is the energy density of the soft photons in the shock rest frame. If eq. (1) is multiplied by a factor of 4/3, one obtains the IC power of a relativistic electron in an isotropic photon field. In the present case, a beam of soft photons illuminates the shock-accelerated electrons along the radial direction. One needs to introduce a correction factor to the IC power in an isotropic photon field (Fan & Piran 2006). This correction combined with the factor 4/3 gives a coefficient of order unity, which is neglected in eq. (1). The peak spectral density (i.e., power per unit energy) is approximated by

$$P_{\epsilon_\gamma,\max} = \frac{P(\gamma_e)}{\epsilon_\gamma(\gamma_e)} = \frac{\sigma_T}{4\pi R^2}\frac{L_0}{\epsilon_0}, \tag{3}$$

which is independent on γ_e and (apparently) on γ. This expression represents the number of scatterings with soft photons per unit time for a certain electron in the Thomson limit. Thus, the peak spectral luminosity is given by

$$L_{\epsilon_\gamma,\max} = N_e P_{\epsilon_\gamma,\max} = \frac{N_e \sigma_T}{4\pi R^2}\frac{L_0}{\epsilon_0}, \tag{4}$$

where N_e is the total number of electrons.

Similar to Sari, Piran & Narayan (1998), if a relativistic electron loses its energy through the IC discussed here, the critical Lorentz factor γ_c above which electrons cool in the observer's time t is defined through $\gamma\gamma_c m_e c^2 = P(\gamma_c)t$, i.e.

$$\gamma_c = \frac{m_e c}{\sigma_T \gamma U'_0 t} = \frac{4\pi m_e c^2 \gamma R^2}{\sigma_T L_0 t}. \tag{5}$$

As usual, we assume that the instantaneous shock-accelerated electron energy distribution follows a power law: $dN_e/d\gamma_e \propto \gamma_e^{-p}$ for $\gamma_e \geq \gamma_m$. If a constant fraction (ϵ_e) of the post-shock energy density goes to electrons, one has $\gamma_m = (m_p/m_e)\epsilon_e[(p-2)/(p-1)]\gamma = 610\epsilon_e g_p \gamma$, where $g_p = 3(p-2)/(p-1)$.

If the cooling time of electrons with Lorentz factor of γ_m is shorter than t (i.e. $\gamma_m > \gamma_c$), the steady electron energy distribution turns out to be $dN_e/d\gamma_e \propto \gamma_e^{-2}$ for $\gamma_c < \gamma_e < \gamma_m$ and $dN_e/d\gamma_e \propto \gamma_e^{-(p+1)}$ for $\gamma_e \geq \gamma_m$. In such a fast cooling regime, the spectral luminosity at ϵ_γ is (e.g. Blumenthal & Gould 1970)

$$L_{\epsilon_\gamma} = \begin{cases} L_{\epsilon_\gamma,\max}(\epsilon_\gamma/\epsilon_c)^{-1/2}, & \epsilon_c < \epsilon_\gamma < \epsilon_m, \\ L_{\epsilon_\gamma,\max}(\epsilon_m/\epsilon_c)^{-1/2}(\epsilon_\gamma/\epsilon_m)^{-p/2}, & \epsilon_\gamma \geq \epsilon_m, \end{cases} \tag{6}$$

where $\epsilon_c \simeq \gamma_c^2 \epsilon_0$ and $\epsilon_m \simeq \gamma_m^2 \epsilon_0$.

On the other hand, if $\gamma_m < \gamma_c$ (slow cooling), the steady electron energy distribution becomes $dN_e/d\gamma_e \propto \gamma_e^{-p}$ for $\gamma_m < \gamma_e < \gamma_c$ and $dN_e/d\gamma_e \propto \gamma_e^{-(p+1)}$ for $\gamma_e \geq \gamma_c$. In this case, the spectral luminosity at ϵ_γ reads

$$L_{\epsilon_\gamma} = \begin{cases} L_{\epsilon_\gamma,\max}(\epsilon_\gamma/\epsilon_c)^{-(p-1)/2}, & \epsilon_m < \epsilon_\gamma < \epsilon_c, \\ L_{\epsilon_\gamma,\max}(\epsilon_c/\epsilon_m)^{-(p-1)/2}(\epsilon_\gamma/\epsilon_c)^{-p/2}, & \epsilon_\gamma \geq \epsilon_c. \end{cases} \tag{7}$$

3. Shock dynamics and emission luminosity

We assume that the luminosity of a relativistic outflow is $L_w(t) \propto t^k$ for $t < t_w$ and $L_w(t) \propto t^{-5/3}$ for $t \geq t_w$, as is suggested by the popular collapsar model for long-duration, soft-spectrum GRBs (MacFadyen, Woosley & Heger 2001). The Lorentz factor of the outflow is $\gamma_w \gg 1$. The comoving proton number density in the outflow rest frame is $n_w = L_w/(4\pi R^2 \gamma_w^2 m_p c^3)$. For simplification, we also assume that a preexisting shell is so slow (as compared with the outflow) that the shell can be considered as being at rest, and its uniform proton number density is n. We assume that the collision happens at an initial radius R_i. Similar to Sari & Piran (1995), the outflow-shell interaction beyond R_i could be described through two shocks, a reverse shock that propagates into the outflow,

and a forward shock that propagates into the shell. There are four regions separated by the two shocks, (1) the unshocked shell, (2) the forward-shocked shell, (3) the reverse-shocked outflow, and (4) the unshocked outflow. The shock dynamics depends on whether the reverse shock has crossed the outflow. It is clear that at two stages, i.e., during and after the reverse-shock crossing, the shock dynamics is different and thus the emission luminosity should also be different. In the following, we discuss these two stages separately.

3.1. During the reverse-shock crossing

As shown by Sari & Piran (1995), if $\gamma_w^2 \gg n_w/n$, the reverse shock is relativistic and the Lorentz factor of regions 2 & 3 measured in the rest frame of region 1 is

$$\gamma_{\rm fs} = \left(\frac{\gamma_w}{2}\right)^{1/2} \left(\frac{n_w}{n}\right)^{1/4} = 3.24 L_{w,50}^{1/8} n_9^{-1/8} (t_3 + t_{i,3})^{-1/4}, \tag{8}$$

where the convention $Q = 10^x \times Q_x$ in cgs units has been adopted and $t_i = t_{i,3} \times 10^3\,{\rm s} \equiv R_i/(2\gamma_{\rm fs}^2 c)$. The shock radius becomes $R = 2\gamma_{\rm fs}^2 ct + R_i \equiv 2\gamma_{\rm fs}^2 c(t+t_i) = 6.3\times10^{14} L_{w,50}^{1/4} n_9^{-1/4} (t_3 + t_{i,3})^{1/2}\,{\rm cm}$. In addition, the Lorentz factor of region 3 measured in the rest frame of region 4 is

$$\gamma_{\rm rs} = \left(\frac{\gamma_w}{2}\right)^{1/2} \left(\frac{n_w}{n}\right)^{-1/4} = 1.54 L_{w,50}^{-1/8} n_9^{1/8} \gamma_{w,1} (t_3 + t_{i,3})^{1/4}. \tag{9}$$

From eq. (5), we calculate the cooling Lorentz factor of the relativistic electrons

$$\gamma_c = 2.0 L_{0,46}^{-1} L_{w,50}^{5/8} n_9^{-5/8} t_3^{-1} (t_3 + t_{i,3})^{3/4}. \tag{10}$$

The characteristic Lorentz factors of the relativistic electrons in regions 2 & 3 are, respectively,

$$\gamma_m = \begin{cases} 20 \epsilon_{e,-2} g_p L_{w,50}^{1/8} n_9^{-1/8} (t_3 + t_{i,3})^{-1/4}, & \text{region 2,} \\ 10 \epsilon_{e,-2} g_p L_{w,50}^{-1/8} n_9^{1/8} \gamma_{w,1} (t_3 + t_{i,3})^{1/4}, & \text{region 3.} \end{cases} \tag{11}$$

for a soft photon source with a black body spectrum and a typical photon energy $\epsilon_0 \sim k_B T \sim 0.16\,{\rm keV}$ (as in GRB 060218), the cooling energy of the scattered photons is

$$\epsilon_c = 0.64 L_{0,46}^{-2} L_{w,50}^{5/4} n_9^{-5/4} \zeta_T t_3^{-2} (t_3 + t_{i,3})^{3/2}\,{\rm keV}, \tag{12}$$

where $\zeta_T = k_B T/0.16\,{\rm keV}$. The characteristic energies of the scattered photons from regions 2 & 3 are, respectively,

$$\epsilon_m = \begin{cases} 64 \epsilon_{e,-2}^2 g_p^2 L_{w,50}^{1/4} n_9^{-1/4} \zeta_T (t_3 + t_{i,3})^{-1/2}\,{\rm keV}, & \text{region 2,} \\ 16 \epsilon_{e,-2}^2 g_p^2 L_{w,50}^{-1/4} n_9^{1/4} \gamma_{w,1}^2 \zeta_T (t_3 + t_{i,3})^{1/2}\,{\rm keV}, & \text{region 3.} \end{cases} \tag{13}$$

The total electron numbers in regions 2 & 3 are $N_{e,2} = 4\pi R^2(2\gamma_{\rm fs}^2 ct)n = 3.1\times10^{54}L_{w,50}^{3/4}n_9^{1/4}t_3(t_3+t_{i,3})^{1/2}$ and $N_{e,3} = N_{e,2}(\gamma_{\rm rs}/\gamma_{\rm fs}) = 1.5\times10^{54}L_{w,50}^{1/2}n_9^{1/2}\gamma_{w,1}t_3(t_3+t_{i,3})$, respectively. From eq. (4), we then obtain the peak spectral luminosities for regions 2 & 3,

$$L_{\epsilon_\gamma,\rm max} = \begin{cases} 2.7\times10^{46}L_{0,46}L_{w,50}^{1/4}n_9^{3/4}\zeta_T^{-1}t_3(t_3+t_{i,3})^{-1/2}\ {\rm erg\,keV^{-1}\,s^{-1}}, & \text{region 2,} \\ 1.3\times10^{46}L_{0,46}n_9\gamma_{w,1}\zeta_T^{-1}t_3\ {\rm erg\,keV^{-1}\,s^{-1}}, & \text{region 3.} \end{cases} \quad (14)$$

According to equations (12)-(14), the spectral luminosities at scattered photon energy ϵ_γ in regions 2 & 3 are

$$L_{\epsilon_\gamma} = \begin{cases} 2.2\times10^{46}L_{w,50}^{7/8}n_9^{1/8}\zeta_T^{-1/2}(t_3+t_{i,3})^{1/4}\epsilon_{\gamma,\rm 1keV}^{-1/2}\ {\rm erg\,keV^{-1}\,s^{-1}}, & \text{region 2,} \\ 1.0\times10^{46}L_{w,50}^{5/8}n_9^{3/8}\gamma_{w,1}\zeta_T^{-1/2}(t_3+t_{i,3})^{3/4}\epsilon_{\gamma,\rm 1keV}^{-1/2}\ {\rm erg\,keV^{-1}\,s^{-1}}, & \text{region 3,} \end{cases} \quad (15)$$

for $\epsilon_c < \epsilon_\gamma < \epsilon_m$, and

$$L_{\epsilon_\gamma} = \begin{cases} 4.9\times10^{47}\epsilon_{e,-2}^{p-1}g_p^{p-1}L_{w,50}^{(p+6)/8}n_9^{-(p-2)/8}\zeta_T^{(p-2)/2}(t_3+t_{i,3})^{-(p-2)/4}\epsilon_{\gamma,\rm 1keV}^{-p/2}\ {\rm erg\,keV^{-1}\,s^{-1}}, & \text{region 2,} \\ 7.5\times10^{46}\epsilon_{e,-2}^{p-1}g_p^{p-1}L_{w,50}^{(6-p)/8}n_9^{(p+2)/8}\gamma_{w,1}^{p}\zeta_T^{(p-2)/2}(t_3+t_{i,3})^{(p+2)/4}\epsilon_{\gamma,\rm 1keV}^{-p/2}\ {\rm erg\,keV^{-1}\,s^{-1}}, & \text{region 3,} \end{cases} \quad (16)$$

for $\epsilon_c < \epsilon_m < \epsilon_\gamma$. Here $\epsilon_{\gamma,\rm 1keV} = \epsilon_\gamma/1\,{\rm keV}$, and the coefficients in eq. (16) have been calculated for $p = 2.5$.

3.2. After the reverse-shock crossing

We assume that the reverse-shock crossing time is $t_w \sim t_i$. After this time, the central engine luminosity is insignificant because it decays as $L_w \propto t^{-5/3}$ (MacFadyen et al. 2001). Although the electrons in region 3 have cooled down, the higher-latitude scattered photons would reach the observer at a later time. This is the well-known curvature effect (Kumar & Panaitescu 2000; Zhang et al. 2006; Wu et al. 2006; Liang et al. 2006). In the relativistic limit, this effect leads to the emission luminosity $L_{\epsilon_\gamma} \propto t^{-(2+\beta)}$ (where β is the spectral index). As argued by Zhang et al. (2006), the temporal index $\alpha = 2+\beta$ conclusion is essentially unchanged by deceleration of region 3. Meanwhile, the forward shock still sweeps up its surrounding shell and its Lorentz factor decreases as $\gamma_{\rm fs} \propto t^{-3/8}$. The cooling Lorentz factor decays as $\gamma_c \propto (\gamma_{\rm fs}U_0' t)^{-1} \propto \gamma_{\rm fs}R^2t^{-1} \propto t^{-7/8}$ (see eq.[5]) and the cooling energy of the scattered photons deccay as $\epsilon_c \propto t^{-7/4}$. The peak spectral luminosity increases as $L_{\epsilon_\gamma,\rm max} \propto N_e R^{-2} \propto R \propto t^{1/4}$. Thus the spectral luminosity at $\epsilon_c < \epsilon_\gamma < \epsilon_m$ decays as $L_{\epsilon_\gamma} = L_{\epsilon_\gamma,\rm max}(\epsilon_\gamma/\epsilon_c)^{-1/2} \propto t^{-5/8}$.

4. Application to GRB 060218

The prompt emission light curves detected by BAT and XRT are presented in Campana et al. (2006): The 15-150 keV luminosity and the 0.3-10 keV luminosity $\sim$ 900 s after the burst increases as $L_{\rm BAT} \propto t^{\alpha_{\gamma,1}}$ with $\alpha_{\gamma,1} \sim 0.3$ and $L_{\rm XRT} \propto t^{\alpha_{x,1}}$ with $\alpha_{x,1} \sim 0.7$, respectively. Subsequently the 15-150 keV luminosity decays as $L_{\rm BAT} \propto t^{\alpha_{\gamma,2}}$ with $\alpha_{\gamma,2} \sim -4.5$, while the 0.3-10 keV luminosity declines slowly as $L_{\rm XRT} \propto t^{\alpha_{x,2}}$ with $\alpha_{x,2}$ with $\alpha_{x,2} \sim -0.6$ until $t \sim 2600$ s, after which the lightcurve declines rapidly as $L_{\rm XRT} \propto t^{\alpha_{x,3}}$ with $\alpha_{x,3} \sim -4.0$. The different light curves detected by BAT and XRT suggest that their corresponding emission could have originated from different regions. In the following, we show that the X-ray emission and γ-ray emission would be produced from regions 2 and 3 in our model, respectively. An example fit to the observational data with our model is displayed in Figure 1.

We first consider the emission luminosity at the peak time $t_{\rm peak} \sim 900$ s. Taking $p \sim 2.5$, $t_i \sim 10^3$ s and $k_B T \sim 0.16$ keV, we calculate the $15-150$ keV luminosity by using the second expression of eq. (16),

$$L_{\rm BAT} = \int_{15\,{\rm keV}}^{150\,{\rm keV}} L_{\epsilon_\gamma} d\epsilon_\gamma \sim 3.3 \times 10^{47} \epsilon_{e,-2}^{1.5} L_{w,50}^{7/16} n_9^{9/16} \gamma_{w,1}^{2.5}\,{\rm erg\,s^{-1}} \sim 1.8 \times 10^{46}\,{\rm erg\,s^{-1}}. \quad (17)$$

Using the first expression of eq. (15), we have the $0.3-10$ keV luminosity

$$L_{\rm XRT} = \int_{0.3\,{\rm keV}}^{10\,{\rm keV}} L_{\epsilon_\gamma} d\epsilon_\gamma \sim 1.7 \times 10^{47} L_{w,50}^{7/8} n_9^{1/8}\,{\rm erg\,s^{-1}} \sim 3.3 \times 10^{46}\,{\rm erg\,s^{-1}}. \quad (18)$$

From eqs. (17) and (18), we find the shell number density and the outflow luminosity at the peak time $t_{\rm peak} \simeq t_w$,

$$n_9 \sim 0.02 \epsilon_{e,-2}^{-3} \gamma_{w,1}^{-5}, \quad (19)$$

$$L_{w,50} \sim 0.3 \epsilon_{e,-2}^{3/7} \gamma_{w,1}^{5/7}, \quad (20)$$

respectively.

Second, we discuss the light curves before $t_{\rm peak}$. Theoretically, the γ-ray and X-ray luminosities increase as $L_{\rm BAT} \propto L_w^{(6-p)/8}$ and $L_{\rm XRT} \propto L_w^{7/8}$, respectively. Considering $L_w \propto t^k$ before t_w, we require $\alpha_{\gamma,1} \simeq (6-p)k/8 \sim 0.3$ and $\alpha_{x,1} \simeq 7k/8 \sim 0.7$, giving $k \sim 0.8$. This indicates that the outflow luminosity increases slowly with time before $t_{\rm peak}$. In the collapsar model, numerical simulations by MacFadyen et al. (2001) indicate that the accretion rate of the fallback disk by the central stellar-mass black hole typically shows a slowly-rising behavior before the well-known $\dot{M} \propto t^{-5/3}$ accretion starts. The outflow luminosity has a similar temporal power because of a nearly constant Blandford-Znajek power efficiency for

the rotating black hole (McKinney 2005). Thus, our fit is consistent with the prediction of the collapsar model.

Third, after t_w, the reverse shock has crossed the outflow and the curvature effect of region 3 leads to the sharp γ-ray luminosity decay, i.e. $L_{\rm BAT} \propto t^{-(2+\beta)} \sim t^{-3.25}$. This is marginally consistent with the steep decay of the γ-ray emission. A larger value of p or a potential spectral break at higher energies would make the curvature effect more consistent with the observed decay. Meanwhile, region 2 could have entered the self-similar solution of Blandford & McKee (1976) and its X-ray luminosity decays as $L_{\rm XRT} \propto t^{-5/8}$. This is in good agreement with the observed value of $\alpha_{x,2}$.

Fourth, we note from Campana et al. (2006) that after ~ 2600 s both the non-thermal component luminosity and the thermal component luminosity decayed rapidly. This steep decay is the result of the combination of the rapid decay of the cocoon emission (Pe'er et al. 2006) and the curvature effect of region 2 after the forward shock has crossed the shell.

Finally, the forward shock, after crossing the slow shell, would sweep into the circum-burst stellar wind and produce a normal afterglow as observed by *Swift* XRT. A single power law light curve of this afterglow indicates that the outflow is not strongly collimated (Fan, Piran & Xu 2006).

5. Conclusions

The abundant multiwavelength prompt emission data of GRB 060218/SN 2006aj make it possible to constrain the prompt emission mechanisms and model parameters in great detail. The data clearly disfavor the conventional internal shock/synchrotron radiation models that predict strong prompt UV optical emission. Instead the data are consistent with a model that invokes inverse Compton scattering off the thermal photons due to shock breakout. The chromatic lightcurve features of the prompt emission require that the prompt BAT-band emission and XRT-band emission are produced in two different regions, and we identify these as a pair of shocks upon the interaction between a relativistic outflow and a preexisting slow shell. Fitting the data with model poses constraints on the physical parameters of the outflow and the shell, in particular, requires a central engine wind with a slowly-increasing luminosity. This behavior is consistent with the prediction of the popular collapsar model.

This work was supported by NASA under grants NNG05GB67G, NNG05GH92G and NNG05GH91G (BZ, ZGD & EWL) and the National Natural Science Foundation of China under grants 10221001 & 10233010 (ZGD) and 10463001 (EWL).

REFERENCES

Blandford, R. D., & McKee, C. F. 1976, Phys. Fluid, 19, 1130

Blumenthal, G., & Gould, R. J. 1970, Rev. Mod. Phys., 42, 237

Brunetti, G. 2000, Astropart. Phys., 13, 107

Campana, S. et al. 2006, Nature, submitted (version 2) (astro-ph/0603279)

Cobb, B. E., Bailyn, C. D., van Dokkum, P. G., & Natarajan, P. 2006, ApJ Letters, submitted (astro-ph/0603832)

Colgate, S. A. 1974, ApJ, 187, 333

Cusumano, G. et al. 2006, GCN Circular 4775

Dai, Z. G., & Lu, T. 2002, ApJ, 580, 1013

Fan, Y. Z., & Piran, T. 2006, MNRAS, in press (astro-ph/0601619)

Fan, Y. Z., Piran, T., & Xu, D. 2006, MNRAS, submitted (astro-ph/0604016)

Kumar, P. & Panaitescu, A. 2000, ApJ, 541, L51

Liang, E. W. et al. 2006, ApJ, in press (astro-ph/0602142)

MacFadyen, A. I., Woosley, S. E., & Heger, A. 2001, ApJ, 550, 410

McKinney, J. C. 2005, ApJ, 630, L5

Mészáros, P., & Rees, M. J. 1999, MNRAS, 306, L39

———. 2001, ApJ, 556, L37

Mirabal, N., Halpern, J. P., An, D., Thorstensen, J. R., & Terndrup, D. M. 2006, ApJ Letters, submitted (astro-ph/0603686)

Modjaz, M. et al. 2006, ApJ Letters, submitted (astro-ph/0603377)

Pe'er, A., Mészáros, P., & Rees, M. J. 2006, ApJ, submitted (astro-ph/0603343)

Pian, E. et al. et al. 2006, Nature, submitted (astro-ph/0603530)

Piran, T. 2005, Rev. Mod. Phys., 76, 1143

Ramirez-Ruiz, E., Celotti, A., & Rees, M. J. 2002, MNRAS, 337, 1349

Rees, M. J. & Mészáros, P. 1994, ApJ, 430, L93

Sari, R., & Piran, T. 1995, ApJ, 455, L143

Sari, R., Piran, T., & Narayan, R. 1998, ApJ, 497, L17

Sollerman, J. et al. 2006, A&A, submitted (astro-ph/0603495)

Tan, J. C., Matzner, C. D. & McKee, C., 2001, ApJ, 551, 946

Wang, X. Y., Li, Z., & Mészáros, P. 2006, ApJ, 641, L89

Wang, X. Y., & Mészáros, P. 2006, ApJ Letters, in press (astro-ph/0603719)

Waxman, E., & Mészáros, P. 2003, ApJ, 584, 390

Wu, X. F., Dai, Z. G, Wang, X. Y., Huang, Y. F., Feng, L. L., & Lu, T. 2006, ApJ, submitted (astro-ph/0512555)

Zhang, B., & Mészáros, P. 2002, ApJ, 581, 1236

———. 2004, Int. J. Mod. Phys. A, 19, 2395

Zhang, B., Fan, Y. Z, Dyks, J., Kobayashi, S, Mészáros, P., Burrows, D. N., Nousek, J. A., & Gehrels, N. 2006, ApJ, in press (astro-ph/0508321)

Zhang, W., Woosley, S. E., & MacFadyen, A. I. 2003, ApJ, 586, 356

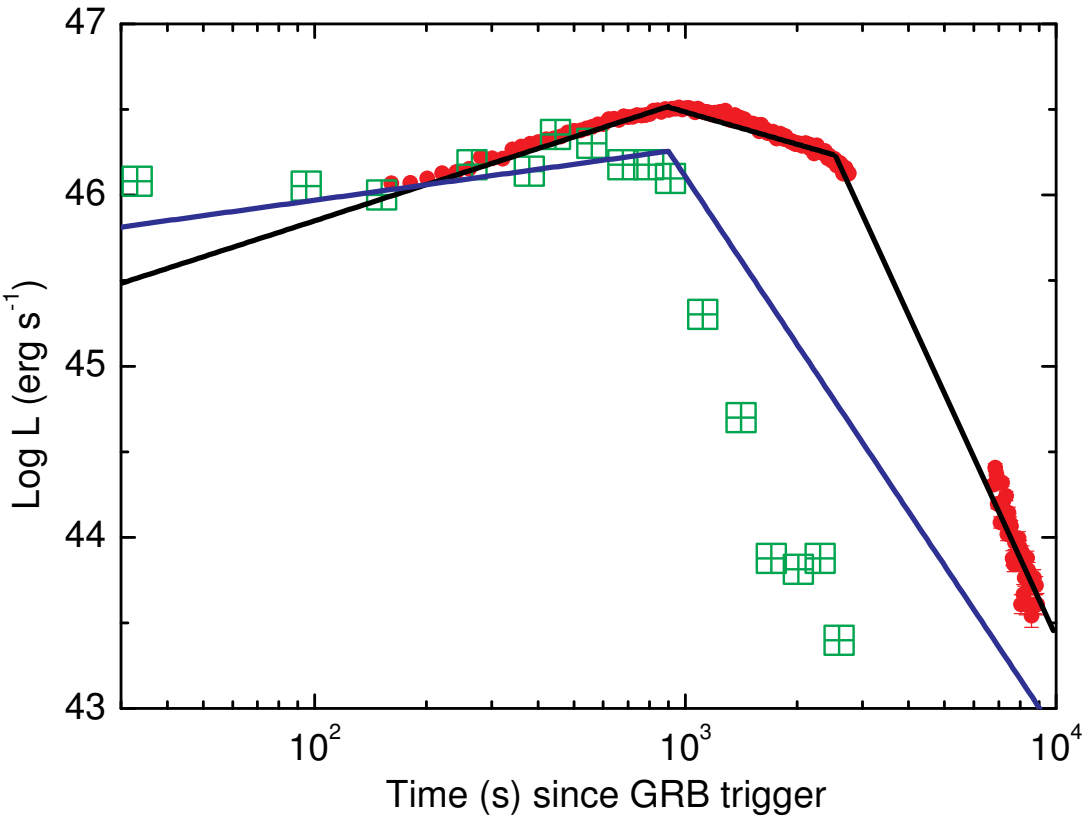

Fig. 1.— An example fit to the prompt emission data of GRB 060218 with our model, for $p \sim 2.5$, $k \sim 0.8$, and $t_w \sim 900$ s. The red dots and green squares represent the XRT and BAT data (taken from version 2 of Campana et al. 2006), respectively. In our fit, the required peak outflow luminosity is $L_{w,50} \sim 0.3\epsilon_{e,-2}^{3/7}\gamma_{w,1}^{5/7}$, the shell number density is $n_9 \sim 0.02\epsilon_{e,-2}^{-3}\gamma_{w,1}^{-5}$, and the shell width is $\Delta R_{\rm shell} \sim 3.2 \times 10^{15}\epsilon_{e,-2}^{6/7}\gamma_{w,1}^{10/7}$ cm. The rising segments of our theoretical γ-ray and X-ray light curves are $L_{\rm BAT} \propto t^{(6-p)k/8}$ and $L_{\rm XRT} \propto t^{7k/8}$, respectively. During the period between $\sim$ 900 to 2600 s, the decaying index of the X-ray luminosity is $-5/8$ and the decaying index of the γ-ray luminosity becomes $-(2+\beta)$ because of the curvature effect after the reverse shock has crossed the outflow. At $\sim$ 2600 s, the forward shock has crossed the shell, and hence, the X-ray luminosity shows a rapid decay due to the curvature effect. However, the actual decay becomes steeper because of the rapid decrease of the observed thermal luminosity.